Modeling suggests SARS-CoV-2 rebound after nirmatrelvir-ritonavir treatment is driven by target cell preservation coupled with incomplete viral clearance

Phan, Tin Thien; Ribeiro, Ruy Miguel; Edelstein, Gregory E.; Boucau, Julie; Uddin, Rockib; Marino, Caitlin; Liew, May Y.; Barry, Mamadou; Choudhary, Manish C.; Tien, Dessie; Su, Karry; Reynolds, Zahra; Li, Yijia; Sagar, Shruti; Vyas, Tammy D.; Kawano, Yumeko; Sparks, Jeffrey A.; Hammond, Sarah P.; Wallace, Zachary; Vyas, Jatin M.; Li, Jonathan Z.; et al.

To be published in: Journal of Virology

DOI to publisher's version: 10.1128/jvi.01623-24

Journal of Virology

| Editor's Pick | Virology | Full-Length Text

Modeling suggests SARS-CoV-2 rebound after nirmatrelvir-ritonavir treatment is driven by target cell preservation coupled with incomplete viral clearance

Tin Phan,[1] Ruy M. Ribeiro,[1] Gregory E. Edelstein,[2] Julie Boucau,[3] Rockib Uddin,[4] Caitlin Marino,[3] May Y. Liew,[4] Mamadou Barry,[4] Manish C. Choudhary,[2] Dessie Tien,[4] Karry Su,[4] Zahra Reynolds,[4] Yijia Li,[2,4,5] Shruti Sagar,[4] Tammy D. Vyas,[4] Yumeko Kawano,[2] Jeffrey A. Sparks,[2] Sarah P. Hammond,[4] Zachary Wallace,[4] Jatin M. Vyas,[4] Jonathan Z. Li,[2] Mark J. Siedner,[4,6] Amy K. Barczak,[3,4] Jacob E. Lemieux,[4,7] Alan S. Perelson[1,8]

AUTHOR AFFILIATIONS See affiliation list on p. 14.

ABSTRACT In a subset of SARS-CoV-2-infected individuals treated with the antiviral nirmatrelvir-ritonavir, the virus rebounds following treatment. The mechanisms driving this rebound are not well understood. We used a mathematical model to describe the longitudinal viral load dynamics of 51 individuals treated with nirmatrelvir-ritonavir, 20 of whom rebounded. Target cell preservation, either by a robust innate immune response or initiation of N-R near the time of symptom onset, coupled with incomplete viral clearance, appears to be the main factor leading to viral rebound. Moreover, the occurrence of viral rebound is likely influenced by the time of treatment initiation relative to the progression of the infection, with earlier treatments leading to a higher chance of rebound. A comparison with an untreated cohort suggests that early treatments with nirmatrelvir-ritonavir may be associated with a delay in the onset of an adaptive immune response. Nevertheless, our model demonstrates that extending the course of nirmatrelvir-ritonavir treatment to a 10-day regimen may greatly diminish the chance of rebound in people with mild-to-moderate COVID-19 and who are at high risk of progression to severe disease. Altogether, our results suggest that in some individuals, a standard 5-day course of nirmatrelvir-ritonavir starting around the time of symptom onset may not completely eliminate the virus. Thus, after treatment ends, the virus can rebound if an effective adaptive immune response has not fully developed. These findings on the role of target cell preservation and incomplete viral clearance also offer a possible explanation for viral rebounds following other antiviral treatments for SARS-CoV-2.

IMPORTANCE Nirmatrelvir-ritonavir is an effective treatment for SARS-CoV-2. In a subset of individuals treated with nirmatrelvir-ritonavir, the initial reduction in viral load is followed by viral rebound once treatment is stopped. We show that the timing of treatment initiation with nirmatrelvir-ritonavir may influence the risk of viral rebound. Nirmatrelvir-ritonavir stops viral growth and preserves target cells but may not lead to full clearance of the virus. Thus, once treatment ends, if an effective adaptive immune response has not adequately developed, the remaining virus can lead to rebound. Our results provide insights into the mechanisms of rebound and can help develop better treatment strategies to minimize this possibility.

KEYWORDS SARS-CoV-2, viral rebound, nirmatrelvir-ritonavir, antiviral therapy, target cell preservation, mathematical model, viral dynamics, adaptive immune response, incomplete viral clearance, treatment timing

Editor Paul G. Thomas, St. Jude Children's Research Hospital, Memphis, Tennessee, USA

Address correspondence to Alan S. Perelson, asp@lanl.gov.

Jonathan Z. Li, Mark J. Siedner, Amy K. Barczak, and Jacob E. Lemieux contributed equally to this article.

A.S.P. owns stock in Pfizer. He was also on a Pfizer advisory committee and received an honorarium. The other authors declare that they have no competing interests.

See the funding table on p. 14.

Received 13 September 2024
Accepted 22 December 2024
Published 4 February 2025

A 5-day course of nirmatrelvir-ritonavir (N-R) is recommended for individuals who test positive for SARS-CoV-2 with mild-to-moderate symptoms and a high risk of progression to severe disease (1). Treatment with two doses (300 mg of nirmatrelvir and 100 mg of ritonavir) per day is suggested to be initiated as soon as possible and within 5 days of symptom onset. Nirmatrelvir is a protease inhibitor, targeting the SARS-CoV-2 main protease 3-chymotrypsin–like cysteine protease enzyme (3CLpro), blocking SARS-CoV-2 replication. Ritonavir reduces the liver catabolism of nirmatrelvir and thus prolongs the half-life of nirmatrelvir (1). Although N-R substantially reduces the risk of progression to severe COVID-19 and can shorten the duration of disease in high-risk individuals (2–4), in some cases, viral rebound and recurring symptoms occur after the 5-day treatment course, including in individuals who have been vaccinated and/or boosted (5, 6). Some individuals with viral rebound are reported to have culturable virus up to 16 days after the initial diagnosis (6, 7); thus, potential transmission to close contacts during the rebound period is a concern (5). Although virus resistance to N-R *in vitro* (8, 9) and treatment-emergent 3CLpro substitutions *in vivo* (1, 10) have been observed, viral rebound in the case of N-R *in vivo* does not seem to be caused by the emergence of drug-resistant mutants (5–7, 11–14). However, two immunocompromised individuals, who were treated with extended duration of N-R in combination with other treatments, experienced viral rebound associated with resistant mutations E166 A/V and L50F in the NSP5 region where 3CLpro is located (15, 16).

The precise proportion of individuals treated with N-R that exhibit viral rebound is unclear, and estimates could vary based on a range of factors, including the definition used to classify rebound and viral characteristics. For example, in the N-R phase 3 clinical trial, EPIC-HR, the fraction of individuals with viral rebound (positive PCR test) and recurring symptoms was 1%–2% (17). However, this study was limited by the relatively infrequent viral RNA measurements after the completion of N-R. Other studies have reported rebound in 0.8%–27% of N-R treated individuals (6, 18–23). Viral rebound has also been described in untreated individuals (24, 25), but often at a lower frequency compared with N-R treated individuals regardless of rebound definition (6, 17, 19, 20, 22, 23, 26, 27).

Throughout the COVID-19 pandemic, viral dynamics models have played an integral part in shedding light on viral infection kinetics, responses to different treatments (28–36), and the implications for epidemiological control (37–39). Moreover, a few studies also analyzed the occurrence of rebounds in untreated (33) and treated infections (40–42). In particular, we previously analyzed the data presented in Charness et al. (5), where quantitative PCR is available for three individuals who experienced viral and symptom rebound after taking N-R. In all three individuals, no resistance mutations in the gene encoding the protease targeted by nirmatrelvir (3CLpro) developed during treatment, and there was no evidence of reinfection by a different variant. The viral dynamic models in our study adequately captured the viral rebound dynamics in all three individuals (43). One hypothesis we tested was that a 5-day N-R treatment course started near the time of symptom onset reduces the depletion of target cells but does not fully eliminate the virus, thus allowing the virus to rebound once treatment is stopped. The occurrence of viral rebound was shown to be sensitive to model parameters, especially the time therapy is started, and the time an adaptive immune response begins to emerge. This suggested that a delay in the treatment initiation can lower the chance of rebound. However, our results were only supported by a limited data set comprised of three individuals (43).

Here, we expand upon this previous study using data from an ongoing observational cohort study, including 51 individuals treated with N-R, 20 of whom were classified as having viral rebound per the definition by Edelstein et al. (6) (additional details in "Data" section, below). Our model accurately captured the viral dynamics of all 51 individuals and provided further evidence that target cell preservation plays a central role in the occurrence of large-amplitude viral rebounds. Our model predicts that target cell preservation was achieved by a robust innate immune response or by early treatment.

As treatment only stops viral replication but does not directly eliminate existing viruses, residual viruses may remain after treatment has ended and can infect the remaining target cells and rebound. Interestingly, our model also suggests that N-R treatment may slightly delay the development of the adaptive immune response. Nonetheless, extending the course of N-R treatment to a 10-day regimen may greatly diminish the risk of rebound. Although we use N-R as a case study, our theory can also explain the viral rebound observed after treatment with molnupiravir (21), another oral antiviral with FDA emergency use authorization, simnotrelvir/ritonavir (44), a protease inhibitor that also targets the SARS-CoV-2 main protease 3CLpro but has a shorter half-life (45) than nirmatrelvir, and VV116 or mindeudesivir (46), an inhibitor of the viral RNA-dependent RNA polymerase that is not inferior to N-R in reducing time to recovery (47).

RESULTS

Model of viral dynamics in the upper respiratory tract

We used an extension of a viral dynamic model that has been applied to study SARS-CoV-2 infection dynamics (28, 29, 32, 41, 48). In this model (depicted in Fig. 1), viral infection of target cells in the upper respiratory tract (URT) occurs with rate constant β. After spending an average time of $1/k$ in an eclipse phase, E, infected cells enter a productively infected state, I, where they produce virus at rate p (in the absence of N-R) and die at per capita rate δ. SARS-CoV-2 is cleared at per capita rate c.

SARS-CoV-2 infection induces both innate and adaptive immune responses (49–52). As in previous models (29, 48, 53, 54), we simplified these responses and focused only on key aspects, such as the induction of an antiviral state by the interferon response that is commonly seen in acute viral infections. Type-I and type-III interferons (IFNs) are produced both by infected cells and innate immune cells, such as plasmacytoid dendritic cells, which are recruited in response to cell infection. Rather than modeling IFN directly, we assumed the amount of type-I and type-III IFN in the URT is proportional to the number of infected cells, I, and that interferon puts target cells into a temporary antiviral state (refractory to infection) (28, 48, 55–58) at rate ϕ. Refractory cells become susceptible to infection again at rate $\rho(I) = \rho\frac{K_\rho}{I+K_\rho}$, where ρ is the maximum rate at which refractory cells return to being susceptible (59), and K_ρ denotes the density of infected cells at which the rate of return is half-maximal. (Note if $I \gg K_\rho$, i.e., if the amount of interferon is very high, $\rho(I) \to 0$, and cells remain in an antiviral state. However, as infection resolves and I becomes much less than K_ρ, the antiviral state is lost at rate close to ρ.) Following Pawelek et al. (60), the adaptive immune response is modeled as causing an exponential increase in the death rate of infected cells (δ) at rate σ for a

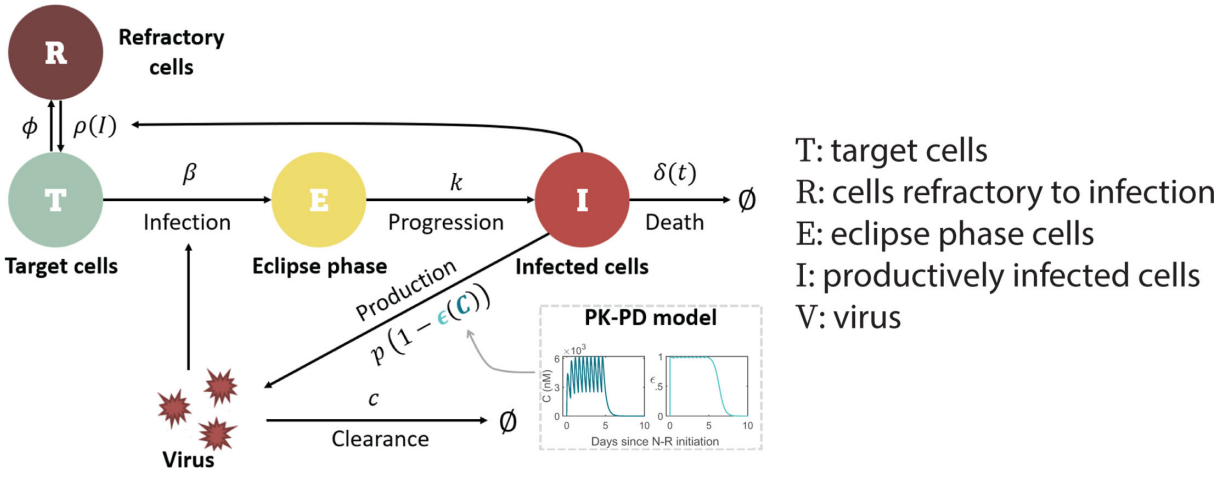

FIG 1 Schematic of the viral dynamic model. The model includes pharmacokinetic (PK) and pharmacodynamic (PD) sub-models, specifying how the drug concentration C and drug effectiveness $\epsilon(C)$ change over time (model details in Materials and Methods and Text S1).

short time after its emergence at time t^*. This choice was motivated by the observation of the exponential expansion of virus-specific $CD8^+$ T cells after SARS-CoV-2 infection (61). Antibodies also increase exponentially shortly before viral control (49) and can contribute to infected cell death via processes such as antibody-dependent cellular cytotoxicity and antibody-dependent cellular phagocytosis. This makes the death rate of infected cells a function of time $\delta(t)$. Finally, the concentration-dependent action of N-R is incorporated using a pharmacokinetic-pharmacodynamic (PK-PD) model. Additional details of the model formulation are provided in Materials and Methods, Text S1, and Fig. S1.

Model describes the viral dynamics in all treated individuals

Our viral dynamic model describes the observed data for treated participants with and without rebound (Fig. 2a). By fitting the model to the data, we obtain population (Table S1 in Text S2) and individual (Table S2 in Text S2) estimates of the model parameters, which are stratified by rebound vs. non-rebound (Fig. 2b). The estimated time of infection relative to the time of symptom onset as reported by participants and the time of N-R initiation relative to infection and to symptom onset are also shown in Fig. 2b. We found that the parameters (ρ, ϕ, and K_ρ) governing the dynamics of refractory cells, that is, those cells that are protected from infection, are significantly different between individuals who rebound and those who do not. The differences in all of these parameters between the two groups were such that they favored the maintenance of cells in the refractory state in non-rebounders, who had a larger rate of cell entry into refractoriness ϕ ($P = 0.0004$), a smaller maximum rate of cells returning to target status ρ ($P = 0.0047$), and a smaller half-saturation constant for this process K_ρ ($P = 0.0056$).

In addition, the baseline infected cell death rate (δ_0) was also significantly lower in non-rebounders ($P = 0.0027$). When we used the previous classification of rebounder or non-rebounder for the participants in this study used by Edelstein et al. (6) and tested "rebounder" as a covariate on each parameter to improve the model fit and better understand factors distinguishing rebounders from non-rebounders, a covariate in δ_0 provided the lowest corrected Bayesian Information Criterion (BICc) (62). However, the BICc difference was small (less than 4 points) compared with the model without a covariate (Table S3 in Text S3). Therefore, we did not include any covariates in the model used to characterize rebound vs. non-rebound (Fig. 2). Additionally, when we considered a variation of our best fit model with proliferation of target cells (details and model fit in Fig. S2a in Text S4), the baseline infected cell death rate was not significantly different between rebounders and non-rebounders (Fig. S2b). On the other hand, there were still differences that are significant in the innate immune response parameters ϕ ($P = 0.0222$) and K_ρ ($P = 0.0201$). Specifically, in both models, the rebounders tend to have a larger value of ϕ, indicating a more rapid loss of target cells by going into the refractory state initially, and a larger value of K_ρ, resulting in an earlier replenishment of target cells that can support viral rebound (40).

The time of N-R treatment relative to the estimated time of infection was about 1 day shorter in participants who rebounded vs. those who did not (median 3.75 days vs 4.72 days, $P = 0.0003$). This is consistent with the significant difference ($P = 0.0009$) in the time of N-R initiation relative to the time of symptom onset in rebound vs. non-rebound individuals, as suggested before (6, 40, 43, 63). These differences in parameter estimates manifest in clear distinctions in model dynamics (viral load, target cells, infected cells) between rebounders and non-rebounders, as discussed and demonstrated in Fig. S3 and S4; Text S5. A model variation that includes logistic proliferation of target cells discussed in Text S4 also predicts similar model dynamics (Fig. S5 in Text S5).

Finally, the model also recapitulates the data in untreated individuals from the same ongoing clinical cohort (Fig. S6a in Text S6). We also find that the parameter distribution between the treated and untreated groups is statistically similar (Fig. S6b in Text S6). The one exception is the average difference of 1.23 days (95% CI [0.44, 2.03], $P = 0.0026$)

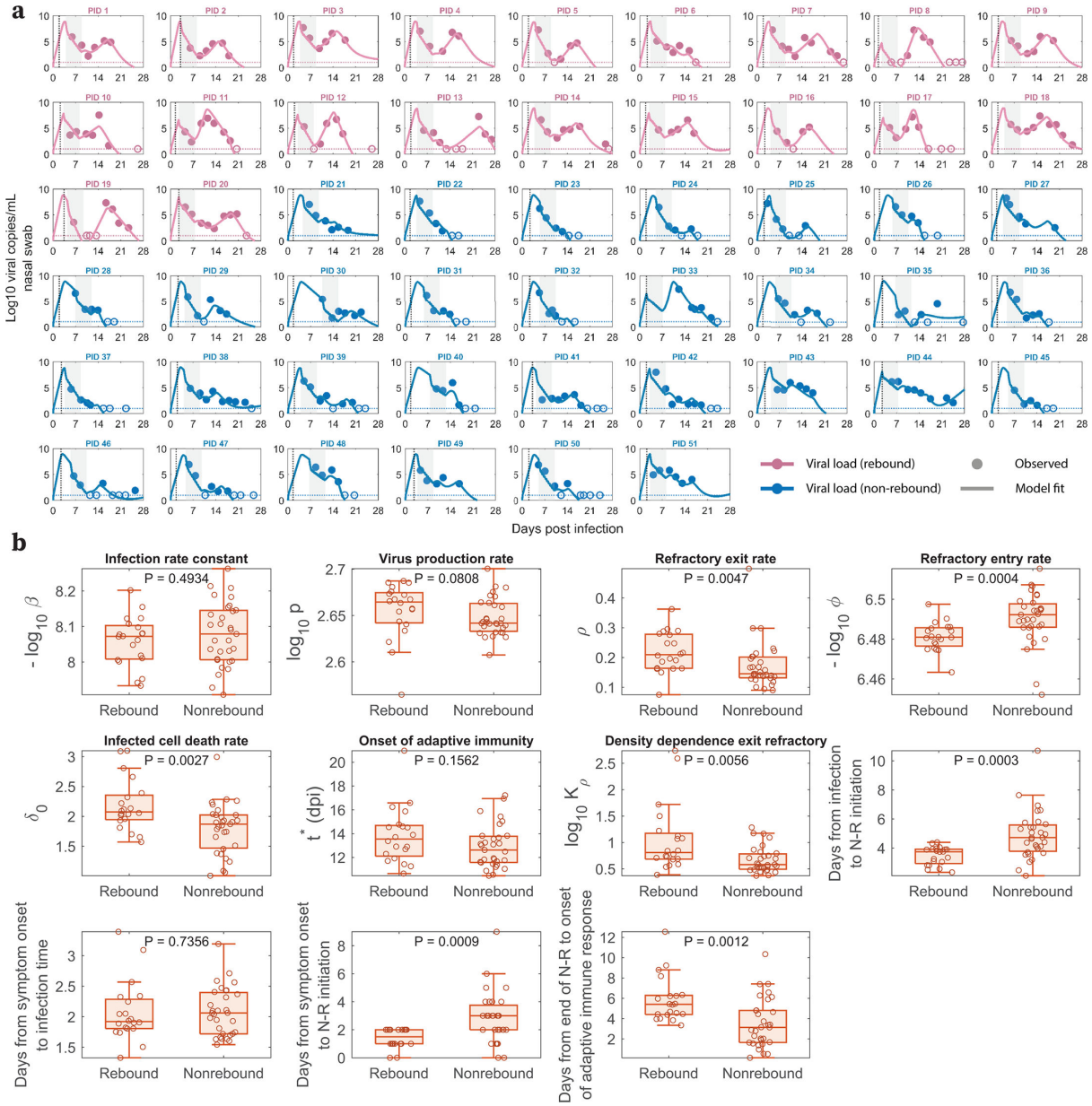

FIG 2 Model fits recapitulate viral dynamics and quantify differences in the characteristics between viral rebound and non-rebound individuals. (a) Model fits to nasal viral loads of rebound (pink) and non-rebound (blue) individuals. The shaded area is the duration of N-R treatment. The dotted horizontal line is the limit of detection (LoD) for the RT-qPCR assay. Filled and open circles are data above and below the LoD, respectively. The dotted black vertical line indicates the reported time of symptom onset relative to the estimated time of infection. (b) Box plots of best fit parameters and timing of N-R stratified by individuals who rebound vs. those who do not. The lower and upper limits of the box represent the first and third quartiles, respectively. The line inside the box is the median, and the whiskers connect the top/bottom of the box to the max/min values that are not outliers (data points further than 1.5 times the interquartile range). Overlaid circles are individual parameter values. Time of N-R initiation relative to symptom onset was recorded for each individual (except non-rebounder PID 23, whose symptom onset is imputed 1 day prior to their first positive test). P-values are calculated using the Mann-Whitney U test.

in the estimated onset time of the adaptive immune response, which is later in treated individuals compared with untreated individuals.

Sensitivity of viral rebound to treatment initiation time and the duration of treatment

Our results suggest that the time of N-R treatment initiation and the availability of target cells at that time are critical to defining whether a rebound occurs. To further explore this, we used simulation experiments to show that delaying or extending the period of treatment with N-R can decrease the probability of rebound. We simulated $n = 20$ treatment cohorts, each with 100 randomly generated *in silico* individuals treated with N-R (see Materials and Methods for details), and assessed what percentage of individuals in each cohort exhibited rebound, defined as the viral load returning above 10^4 RNA copies per mL (6). Samples of the simulated viral dynamics for individuals in the *in silico* cohorts are presented in Fig. S7a-c in Text S8. Without treatment, our cohorts of *in silico* individuals have similar rebound statistics as those reported in the eight clinical studies (6, 17, 19, 20, 24–27) (Fig. S7d in Text S8).

We tested treatment starting at days 1, 2, 3, and 4 post-symptom onset, with symptom onset assumed to be 3 days post-infection. Extending treatment could be a feasible method of preventing rebound (40, 43, 64); hence, we also examined a 5-, 6-, 7-, 8-, and 10-day treatment courses. In one scenario, we assume N-R does not affect the development of adaptive immune response (Fig. 3). In a second scenario, we assume that the onset of the adaptive immune response is delayed more with longer treatments (Fig. S8 in Text S9). It is important to examine this possibility as it would make rebound more likely. The time of symptom onset is fixed at 3 days post-infection; however, assuming either 2 or 4 days does not change the general trend observed in Fig. 3 and Fig. S8 in Text S9 in which we observed a clear decrease in rebound percentage as treatment is initiated later. We also found that an increase in the duration of treatment with N-R tends to prevent viral rebound. In all scenarios, extending treatment to 10 days decreases the probability of rebound in our 20 simulated 100-person cohorts to a level so low that it does not occur for all practical purposes.

DISCUSSION

Here, we extended a viral dynamic model of SARS-CoV-2 infection to show that the main driver of viral rebound in the setting of treatment is the preservation of target cells, often as a result of a robust innate immune response or early treatment initiation. Our model shows that if N-R treatment is completed and the drug is washed out before an adaptive immune response develops, residual viable viruses can rebound if there are sufficient target cells remaining. These results support our initial hypothesis of the importance of target cell preservation and the time therapy is initiated in leading to viral rebound (43), and they also echo the findings of a modeling study by Esmaeili et al. (40) based on data

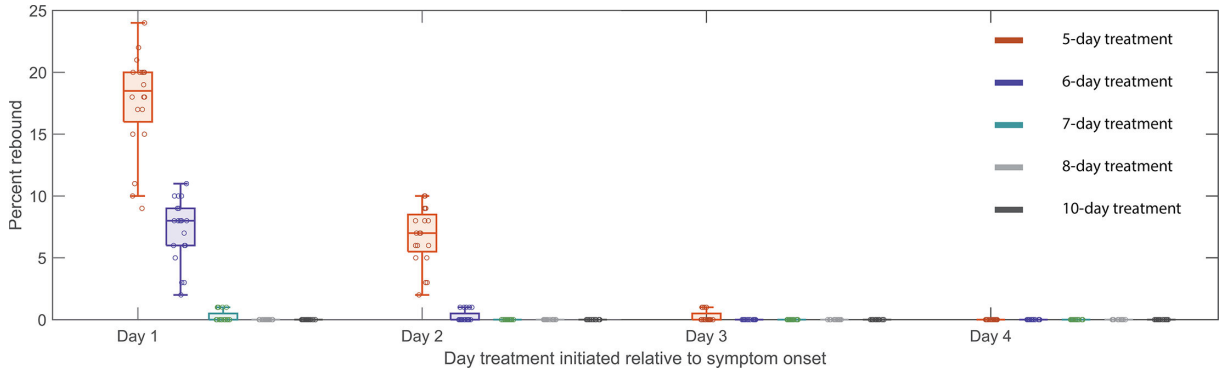

FIG 3 Predicted rebound relative to the time and duration of treatment. Predicted rebound for 5-, 6-, 7-, 8-, and 10-day courses of N-R. Symptom onset is assumed to occur 3 days post-infection. Boxplots depict the percentage of rebound cases from 20 *in silico* cohorts, each with 100 individuals, for different treatment initiation times. Each open circle represents the rebound percentage from one cohort. The extended duration of N-R (beyond a 5-day treatment course) is assumed to not cause additional delay on the onset of the adaptive immune response.

from the EPIC-HR and PLATCOV clinical trials, highlighting the robustness of these results obtained with different models and using different data sets.

Our best model is able to capture the viral dynamics observed in all participants. It suggests that the protective effects of innate immunity preserved the majority of target cells by putting them into an antiviral state shortly after the virus started growing exponentially (Fig. S3 and S4 in Text S5). During treatment, the viral load and the number of infected cells rapidly decline (Fig. 2a; Fig. S4c, f in Text S5) due to infected cell death and continuous viral clearance, concurrent with reduced viral production due to drug activity. This decline leads to a decrease in the interferon response, causing cells to exit more quickly from the refractory state (55–59). It is clear from the data of both rebound and non-rebound individuals that a 5-day course of N-R is likely to be insufficient to completely eliminate the virus. Indeed, there was a measurable virus (viral load >LoD) after the completion of treatment (the first data point after treatment) in 40 of the 51 participants (Fig. 2a). Thus, if viable viruses remain after the drug is washed out and before an adaptive immune response can be mounted, virus can rebound. However, whether the virus rebounds to an observable level is also determined by the time between the end of treatment and the generation of an effective adaptive immune response, and to some degree, the differences in the maintenance of the cell refractory status (Fig. 2b). This conclusion is supported by the observation that the time between the end of treatment and the predicted onset time of an adaptive immune response in the model is statistically different between the rebound and non-rebound groups. For the rebound group, the estimated time [min, max] is 5.87 [3.34, 12.56] days, and for the non-rebound group, it is 3.53 [0.14, 10.35] days (P = 0.0012) (Fig. 2b). Note that this difference is not driven by the fitted onset time of the adaptive immune response t^* measured from the estimated time of infection, whose distribution is statistically similar between the two groups (Fig. 2b). Instead, the difference in the time between the end of treatment and the onset time of the adaptive immune response is mainly driven by the earlier time of treatment initiation in the rebound group (Fig. 2b).

The time of treatment initiation also plays a crucial role in determining if a rebound is observed, as was also seen by Esmaeili et al. (40). If treatment is initiated early after infection, before a time we denote $t_{critical}$, a substantial number of target cells remain unprotected after the 5-day treatment and viral rebound is likely to occur. After $t_{critical}$, too few target cells remain available to support viral growth; however, target cells still return from the refractory state as the virus is eliminated. Since viral growth switches to viral decay at the time of the viral peak in an untreated individual, this means $t_{critical}$ is the time the viral peak is reached. In more technical terms $t_{critical}$ corresponds to the time the effective reproductive number $\Re$ equals 1, so that on average, each infected cell produces one new infected cell, leading to neither growth nor decay in the number of infected cells. In several observational/retrospective studies focusing on Omicron subvariants, the time to the viral peak is suggested to be 2–5 days post-symptom onset (65–67). We observed that for the participants in this study, who were all infected with Omicron subvariants, rebound is associated with treatment initiated within 2 days of symptom onset (6). This suggests treatment might have been initiated prior to $t_{critical}$, when the virus level is still expanding. Delaying treatment may be a strategy to reduce the possibility of viral rebound (Fig. 3; Fig. S8 in Text S9); however, delaying treatment could have a negative impact on the severity of disease in the high-risk individuals for whom N-R is recommended, and this question deserves more study (37). In addition, N-R treatment accelerates viral clearance and hence potentially can reduce viral transmission. See Fig. 4 for a summary description of our results.

Interestingly, all individuals studied here were vaccinated and boosted, and nonetheless had breakthrough infections with Omicron sub-variants (6). Thus, although adaptive B and T cell immune responses did not prevent infection, they might have been present at the time of infection and could have affected the level of preserved target cells. The timing of the adaptive immune response and its expansion may play a crucial role in the occurrence of viral rebound. In particular, without a strong adaptive immune response,

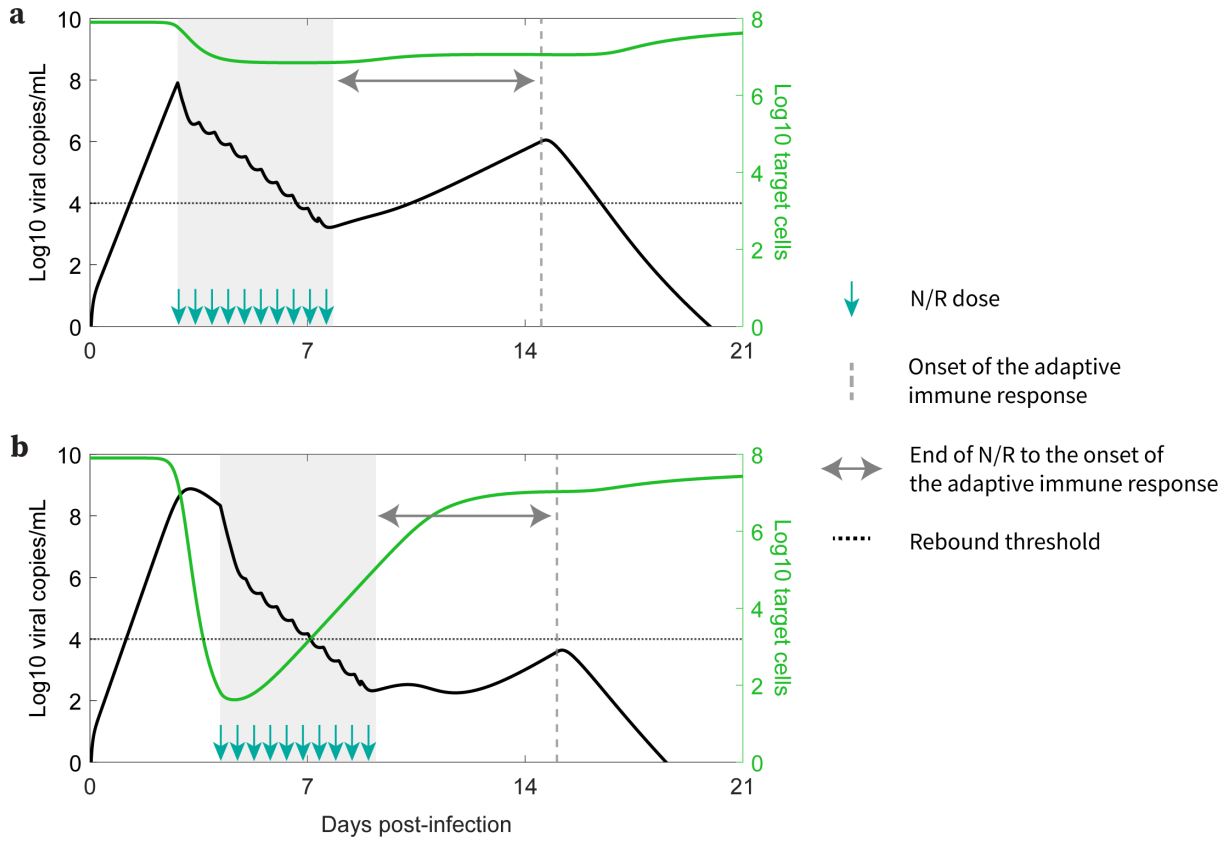

FIG 4 How early treatment correlates with higher rebound probability. (a) Early treatments preserve more target cells and result in a longer duration between the end of N-R and the onset of an adaptive immune response, leading to a higher probability of an individual being classified as experiencing a rebound. (b) Later treatments preserve fewer target cells and result in a shorter duration between the end of N-R and the onset of an adaptive immune response, leading to a lower probability of an individual being classified as experiencing rebound.

even a longer course of N-R still resulted in viral rebound in immunocompromised patients with severe disease (15, 16, 68). Delaying the initiation of N-R may also provide more time for the priming of the adaptive immune response and shorten the time between the end of treatment and the emergence of the adaptive immune response, which would reduce the chance of rebound.

Our model predicted that the 20 rebound participants in the studied set have both innate and adaptive immune responses comparable with those of non-rebound participants (Fig. 2b). This intriguing finding is supported by the clinical observations that most viral rebounds quickly resolve within several days (69), and this correlates with a strong antibody and T-cell immune response (13). There is also contradictory evidence suggesting that N-R may delay the development of the adaptive immune response (70, 71). We found an average of 1.23 day delay in the estimated onset time of the adaptive immune response in the treated vs. untreated groups (Text S6). Even so, the rebound participants quickly cleared the rebounding virus. This suggests that although early initiation of N-R may slightly delay the onset of the adaptive immune response, perhaps due to lower levels of antigens, it does not stop the development of an adaptive immune response in non-immunocompromised individuals. Thus, if the adaptive immune response is not significantly impeded by treatment, prolonging treatment can be beneficial in reducing rebound and does not have the possible detrimental effects on disease severity or increase viral transmission by delaying treatment (63). Indeed, using an *in silico* cohort, we show that even a modest extension to a 6-day treatment course can significantly reduce viral rebound incidence (Fig. 3; Fig. S8 in Text S9). Extensions beyond a 6-day treatment course can further reduce rebound

incidence with a 10-day treatment course almost totally eliminating the possibility of rebound in our *in silico* patient cohorts (Fig. 3; Fig. S8 in Text S9). A recent clinical trial compared 5 vs. 10 vs. 15 days of treatment with N-R given to immunocompromised patients with COVID-19 (ClinicalTrials.gov: NCT05438602). The final analysis of 150 participants showed that extending treatment to 10 or 15 days can minimize the risk of rebound (72). Although 9 of 52 participants treated with 5 days of N-R rebounded, only one participant rebounded in the 10-day (n = 48) and 15-day (n = 50) treatment groups. Although the clinical trial was carried out with immunocompromised patients, the single rebound incidence in the 10-day treated group supports our simulation results for a theoretical 10-day treatment for mild-to-moderate individuals with a high risk of progression (Fig. 3). When the cost of the drug is accounted for, the optimal treatment duration to minimize rebound and cost falls between 7 and 8 days (Fig. S9 in Text S10). However, because N-R is packaged as a 5-day course of treatment, extending treatment to 10 or 15 days may be more practical. Additionally, we previously suggested that the success of a second course of N-R once viral rebound occurs will also depend on the timing of an effective adaptive immune response in a similar manner (43). This is corroborated by observations of recurring viral rebounds in an immunocompromised individual at the end of each treatment period, which eventually leads to the development of the resistance mutation E166V/L50F (15). An ongoing clinical trial aims to investigate this possibility (ClinicalTrials.gov: NCT05567952).

Rather than extend treatment duration, the use of a drug with a longer half-life may be helpful, especially if infectious forms of SARS-CoV-2 can persist during antiviral treatment (8, 9, 73). An ongoing clinical trial of ensitrelvir (ClinicalTrials.gov: NCT05305547) (74), a protease inhibitor that also targets SARS-CoV-2 3CLpro but with a longer half-life than nirmatrelvir (75), yielded results suggesting that this new drug was virologically active and did not significantly increase the risk of viral rebound (64).

The phenomenon of viral rebound has also been observed for monoclonal antibody treatments for SARS-CoV-2 (76–80). One example is bamlanivimab, the first monoclonal antibody that received FDA emergency use authorization for the treatment of COVID-19 (78–80). However, rebounds in the case of monoclonal antibodies are associated with the emergence of resistance mutations (76–80), which contrasts with the lack of evidence for resistant mutants *in vivo* in the majority of cases for the current antiviral treatments (5–7, 11–13). However, the emergence of resistance mutations to monoclonal antibodies does not always lead to viral rebound (76, 77), suggesting other mechanisms besides selection pressure due to treatment may contribute to observable viral rebounds. Our previous modeling studies suggested that target cell regeneration mechanisms, such as homeostatic proliferation of epithelial cells (81–83) or refractory cells returning to a susceptible state, are necessary to explain the high amplitude viral rebounds observed in bamlanivimab treated participants (41). Here, our model with logistic proliferation (Text S4) also recapitulates the viral load dynamics in rebound and non-rebound participants (Fig. S2a in Text S4), and the stratified parameter values also support the conclusion that early N-R initiations correlate with a higher probability of rebound (Fig. S2b in Text S4). However, the net regeneration effect of target cells is similar to that in the innate immune response model (Fig. S5 compared with Fig. S3 in Text S5). This is likely because potent target cell preservation limits the proliferation rate, which is related to the number of cells that are lost by infection and need to be replaced. Moreover, because rebound occurs within days after the end of treatment, there is also not sufficient time for the proliferation effect to be more evident. In addition to explaining viral rebound, target cell regeneration mechanisms may also explain the observations of low-amplitude viral rebounds/persistence in untreated individuals prior to the development of an effective adaptive immune response (84, 85).

Our study has some limitations, the principal of which is not knowing the precise date of infection of each individual. This is a very common situation when dealing with infectious diseases (86, 87), and it is ameliorated by using well-established viral dynamical models (29, 32, 33, 48), which in most cases allow us to infer the time of

infection better than may be known clinically. Another important issue is that we do not have data on the immune response in the study participants, although we include both innate and acquired immune factors in our model. In the context of vaccinated individuals, this could be even more important, although it has been shown before that the viral dynamics of breakthrough infections may be similar to that in unvaccinated individuals (88, 89). Our study could be strengthened and validated by incorporating detailed longitudinal immune response data, similar to those collected in the human challenge study for SARS-CoV-2 (49). Furthermore, for the logistical proliferation model, markers of target cell proliferation or re-population could be used to support the model. We should also re-emphasize that although delaying treatment leads to a lower probability of rebound, we do not evaluate the effect on the severity of the disease.

In summary, our results suggest the occurrence of viral rebound following a complete course of N-R may be due to the level of preserved target cells in the setting of incomplete elimination of the virus. Delaying initiation of treatment for a day or a few days following the first signs of infection should have some benefit in reducing the possibility of rebound, but at the cost of allowing viral growth to continue and the possibility of increased disease severity. On the other hand, extending treatments by several days may also reduce the likelihood of rebound, but at an increased cost of the drug. We remark that viral rebound is not an intrinsic feature of our model, but rather a possibility within the model dynamical landscape. This is clearly demonstrated by the model fits to non-rebound individuals (treated and untreated). Finally, rebound following antiviral treatments is not unique to N-R (21, 44). In particular, rebound without evidence of resistance has also been observed for the protease inhibitor simnotrelvir (44), which has a similar mechanism of action to nirmatrelvir and a shorter half-life (45). Thus, these findings may provide an explanation for rebound following other antiviral treatments besides N-R.

MATERIALS AND METHODS

Data

The data in this study come from an ongoing observational cohort study. Full details of the study design and observations have been reported previously (6). In summary, participants are adult outpatients selected from those who took part in the POSITIVES study (Post-vaccination Viral Characteristics Study) (7, 90) within 5 days of an initial positive diagnostic test for COVID-19, had not yet completed a 5-day course of N-R, and had not received other antiviral or monoclonal antibody treatments (6). Time of symptom onset was reported by participants and infection was confirmed with an initial PCR or rapid antigen test. Anterior nasal swabs were self-collected about three times a week for 2 weeks, then weekly until persistent undetectable results. The data were originally reported relative to the time of the initial diagnostic test (6); however, we shifted the data to be "Days post-infection" (Fig. 3) based on fitting the model to the data (see Data Fitting). The primary definition for viral rebound was either (a) a positive viral culture following prior negative results, or (b) nadir viral load dropping below 4 log10 copies/mL, then increased by at least 1 log10 copies/mL above the nadir and sustained above 4 log10 copies/mL for two consecutive measurements (6).

For this analysis, we selected all participants who took N-R and met two criteria: (i) had at least five data points, with (ii) at least 4 of those data points above LOD. There were 51 participants that met these criteria (20 showing rebound and 31 showing no rebound).

Details regarding the statistics of rebound in untreated individuals are presented in Table S4 in Text S7.

Mathematical model

We used an extension of the viral dynamic model, originally developed by Baccam et al. (91), Saenz et al. (92), and Pawelek et al. (60) to study acute influenza infections, which

has previously been adapted to study SARS-CoV-2 infection dynamics (28, 32, 41, 48). The model below statistically outperformed the simpler versions used by Perelson et al. (43) (see Table S3 in Text S3). Iyaniwura et al. (29) recently studied the kinetics of SARS-CoV-2 infection using a variation of this model that considers both infectious and total virus.

Our model is described by the following set of ordinary differential equations:

$$T' = -\beta VT - \Phi IT + \rho\frac{K_p}{I+K_p}R$$

$$R' = \Phi IT - \rho\frac{K_p}{I+K_p}R$$

$$E' = \beta VT - kE$$

$$I' = kE - \delta(t)I$$

$$V' = (1-\epsilon(C))pI - cV$$

In this model, T is the number of target cells in the URT, E is the number of infected cells that have not yet started to produce virus, that is, are in the eclipse phase, I is the number of productively infected cells, and V is the viral load. Target cells become infected with rate constant β. After being infected for an average time of $1/k$, infected cells in the absence of therapy start producing virus at an adjusted rate p that accounts for sampling via a swab (28, 48) and die at per capita rate δ, which we allow to be time dependent as described below. SARS-CoV-2 is cleared at per capita rate c. The viral production rate, baseline infected cell death rate, and viral clearance rate are influenced by the innate immune response. For example, NK cells can eliminate infected cells, thereby contributing to the infected cell death rate. Activation of the complement system enhances viral clearance, affecting the viral clearance rate. Additionally, the release of cytokines, chemokines, and antiviral restriction factors could have an effect on viral production and promote the clearance of infected cells. However, the specific actions and distinct effects of the innate immune response components are not explicitly modeled here beyond the effects of type-I and type-III interferons.

For the innate immune response, we assume (48, 60) the level of type-I and type-III interferons in the URT is proportional to the number of infected cells, *I*, because these cells produce IFN and recruit other IFN-producing cells, such as plasmacytoid dendritic cells. We also assume that interferon puts target cells in an antiviral state that is refractory to infection at rate ϕ (55–58). The number of cells refractory to infection is denoted as R. Refractory cells lose their protection and become susceptible to infection (59) at a rate $\rho\frac{K_\rho}{I+K_\rho}$. The density dependence of this rate on the number of infected cells I reflects the idea that when infected cells are abundant, they stimulate a strong interferon response, which keeps uninfected cells in a refractory state; but when infected cells decay below a critical threshold, they no longer sustain a sufficient interferon response to maintain cells in a refractory state and these cells return to being susceptible again (55–59). Note that promoting a refractory state is just one possible mechanism of the innate immune system to fight SARS-CoV-2 infection (93). A previous study by Ke et al. (48) examined various formulations (e.g., reduction in infection or viral production rate) that reflect different mechanisms of the innate immune response and found this formulation to be superior in capturing viral dynamics data.

We added to this model an adaptive immune response, since rebounds tend to occur late after infection, when adaptive immune responses have been observed (13).

As modeled by Pawelek et al. (60), we added this response to the model starting at time t^*. We assumed that the adaptive response increases exponentially at rate σ for the short time period we model and causes an increase in the death rate of infected cells. This increased death rate could be due to the increasing presence of cytotoxic T cells or of viral-specific antibodies that bind to infected cells and cause their death by processes such as antibody-dependent cytotoxicity, antibody-dependent phagocytosis, or complement-mediated death. For simplicity, we fixed $\sigma = 0.5$ per day, which means that 1, 2, 3, and 5 days after t^*, the adaptive immune response will be at approximately 45%, 67%, 80%, and 93% of its maximum strength. The time-dependent infected cell death rate $\delta(t)$ takes the form:

$$\delta(t) = \begin{cases} \delta_0 & \text{for } t < t^* \\ \delta_m - (\delta_m - \delta_0)e^{-\sigma(t-t^*)} & \text{for } t \geq t^* \end{cases}$$

The effectiveness of nirmatrelvir in blocking viral replication and subsequent production of virions is given by $\epsilon(C) = \epsilon_{max}\frac{C}{C + EC50}$, an E_{max} model (94) where C is the concentration of nirmatrelvir, EC_{50} is the concentration at which the drug effectiveness is half-maximal, and ϵ_{max} is the maximum effectiveness. When $\epsilon(C) = 0$, the drug has no effect, and when $\epsilon(C) = 1$, the drug is 100% effective at blocking virion production. Based on the complete model, viral growth occurs only when the fraction of remaining target cells is above a critical threshold, which is $\frac{\delta(t)c}{\beta p(1-\epsilon(C))T(0)}$, corresponding to the effective reproduction number $\Re$ being larger than 1.

As it is impossible to know the number of viruses that initiated infection, we use a method suggested by Smith et al. (95) in which we assume the initiating virus is either cleared or rapidly infects cells. Thus, for initial conditions, we use: $T(0) = 8 \times 10^7$ cells, $E(0) = 1$ cell, $I(0) = 0, V(0) = 0$, and $R(0) = 0$ as explained in Ke et al. (48). They also noted that the infection dynamics are relatively insensitive to increasing the initial number of infected cells to 10.

Pharmacokinetic and pharmacodynamic models for N-R

We assume the drug effectiveness $\epsilon(C)$ depends on the concentration of nirmatrelvir, $C(t)$, according to an E_{max} model with EC50 = 62 nM, as presented in the FDA Emergency Use Authorization (1). In S3 text, we explore the possibility that the *in vivo* EC50 may differ from the *in vitro* EC50 of 62 nM (12, 40). However, estimating the *in vivo* EC50 and its individual variability only slightly improves the model fit but worsens the BICc score as additional parameters are fit (Table S3). Due to the lack of individual PK data, we also could not estimate the *in vivo* EC50 directly. Thus, for the analysis in the main text, we assume the EC50 value reported by the FDA. Following a *single dose* of 300 mg nirmatrelvir with 100 mg ritonavir, the observed maximum nirmatrelvir concentration is $C_{max} = 2.21\frac{\mu g}{mL}$ (1). As nirmatrelvir has a molecular weight (96) of $499.54\frac{g}{mol}$, this value of C_{max} can also be expressed as $4.4 \times 10^3 nM$. The half-life of nirmatrelvir when taken with ritonavir is about 6 h (1), which corresponds to an elimination rate of 2.8 /day. Additionally, dosing twice-daily achieved steady state on day 2 with approximately 2-fold accumulation (1). Using a simple multidose absorption-elimination model, the pharmacokinetics of nirmatrelvir is given by (94)

$$C(t) = \frac{\hat{C}\frac{k_a}{k_e - k_a}\left(\frac{e^{-k_e t}}{e^{k_a I_d} - 1}\right)}{\left[1 - e^{(k_e - k_a)t}\left(1 - e^{N_d k_a I_d}\right) + \left(e^{k_e I_d} - e^{k_a I_d}\right)\left(\frac{e^{(N_d 1)k_e I_d} - 1}{e^{k_e I_d} - 1}\right) - e^{((N_d - 1)k_e + k_a)I_d}\right]}.$$

Here, k_e is the elimination rate (2.8 /day), k_a is the absorption rate (17.5 /day), I_d is the dosing interval (1/2 day),and $N_d = integer\left(\frac{t}{I_d}\right) + 1$ is the number of doses until time t, with the first dose at time $t = 0$. In Text S1, we estimate $\widehat{C} = \frac{FD}{V_d} = \left(6.25 \times 10^3\ \mathrm{nM}\right)$.. Details on the implementation of the pharmacokinetic model and the parameter values used can be found in Text S1. With these assumptions, the drug effectiveness $\epsilon(C)$ hovers around 0.98 during treatment and then falls to zero rapidly after treatment stops (Fig. S1 in Text S1).

Data fitting

We used a nonlinear mixed effects modeling approach (software Monolix 2023R1, Lixoft, SA, Antony, France) to fit the model to viral load data for all 51 individuals simultaneously. We applied left censoring to data points under LOD.

We assumed that the parameters p, δ_0, time of infection, and K_ρ follow a log-normal distribution. Parameters -$\log_{10}$ ϕ, -$\log_{10}$ $\beta, \rho,$ and t* were assumed to follow a logit-normal distribution, with ranges closely following literature values (28, 48). We constrained $-\log_{10}\beta$ between 7.5 and 9. Parameter ρ was constrained between 0 and 1 per day, $-\log_{10}\phi$ between 5 and12, and t* between 7 and 28 days. No covariate was used during the initial fitting. A covariate based on whether a participant is classified as rebound or non-rebound was used later with the best fit model to determine the parameters that are different between these two groups.

The viral load data were originally reported relative to the number days since the initial PCR confirmation test. To estimate the time of infection, we shifted the data to be relative to the reported time of symptom onset. We then estimated the interval from the time of infection, or more precisely the time interval from when virus begins to grow exponentially as estimated by our model fitting, to when the participant reported symptoms. We then shifted the viral load data to be relative to this estimated time of infection.

The process to optimize the initial guesses of fitting parameters was done manually within the given parameter ranges to avoid unrealistic model dynamics. Whenever two models share a fitting parameter, the same initial guess for that parameter would be used in the fitting of both models. Model comparisons were done using the BICc (62) as reported by Monolix.

Construction of an *in silico* cohort

To quantify the chance of viral rebound after a 5-day (or longer) course of treatment with N-R, we simulated a cohort of *in silico* patients. We used the following selection criteria to construct the cohort of *in silico* patients with typical viral load patterns: (i) the viral load must peak above 10^6 copies per mL; (ii) the peak must be reached between days 2 and 7 after infection; and (iii) the viral load must decline below 10^2 copies per mL by day 28. This algorithm is akin to a rejection algorithm, where we sample each parameter from the best fit population estimates (i.e., the estimated distribution) and only accept parameter sets that satisfy conditions (i) – (3). We fixed the time the adaptive immune response starts, t*, to the population estimate of 13 days, and set δ_m = 20 /day to prevent unrealistic rebound once an effective immune response has been developed. Additional details of the *in silico* cohort are presented in Text S8.

We used these admissible parameter sets to simulate treatment of different durations (5, 6, 7, 8, and 10 days of N-R) starting at different times (1–4 days post-symptom onset) and calculate the probability of rebound. We also examined how a potential delay in the development of the adaptive immune response with longer treatment may affect the likelihood of rebound (Text S9).

ACKNOWLEDGMENTS

We thank Ruian Ke and Jeremie Guedj for helpful comments on the manuscript.

This work was performed under the auspices of the US Dept. of Energy under contract 89233218CNA000001 and supported by National Institutes of Health grant U54-HL143541-04 (R.M.R.); Los Alamos National Laboratory LDRD 20200743ER (R.M.R.), 20200695ER (A.S.P.), 20210730ER (R.M.R.), and 20220791PRD2 (T.P.); Massachusetts Consortium on Pathogen Readiness (J.Z.L., J.E.L., A.K.B., and M.J.S.); Massachusetts General Hospital Department of Medicine (J.M.V., A.K.B., and M.J.S.); National Institutes of Health grant U19 AI110818 (J.Z.L., J.E.L., A.K.B., and M.J.S.); and National Institutes of Health grant R01 AI176287 (J.Z.L., J.E.L., A.K.B., and M.J.S.).

Conceptualization: A.S.P., R.M.R., T.P., J.Z.L., M.J.S., A.K.B., and J.E.L. Data curation: G.E.E., J.B., R.U., C.M., M.Y.L., M.B., M.C.C., D.T., K.S., Z.R., Y.L., S.S., T.D.V., Y.K., J.A.S., S.P.H., Z.W., J.M.V., J.Z.L., M.J.S., A.K.B., and J.E.L. Methodology: A.S.P., R.M.R., and T.P. Investigation: A.S.P., R.M.R., T.P., J.Z.L., M.J.S., A.K.B., and J.E.L. Visualization: T.P. Funding acquisition: A.S.P., R.M.R., T.P., J.M.V., J.Z.L., M.J.S., A.K.B., and J.E.L. Project administration: A.S.P., R.M.R., J.Z.L., M.J.S., A.K.B., and J.E.L. Supervision: A.S.P., R.M.R., J.Z.L., M.J.S., A.K.B., and J.E.L. Writing – original draft: T.P. Writing – review & editing: A.S.P., R.M.R., T.P., G.E.E., J.B., R.U., C.M., M.Y.L., M.B., M.C.C., D.T., K.S., Z.R., Y.L., S.S., T.D.V., Y.K., J.A.S., S.P.H., Z.W., J.M.V., J.Z.L., M.J.S., A.K.B., and J.E.L.

AUTHOR AFFILIATIONS

[1]Theoretical Biology and Biophysics, Los Alamos National Laboratory, Los Alamos, New Mexico, USA
[2]Department of Medicine, Brigham and Women's Hospital, Harvard Medical School, Boston, Massachusetts, USA
[3]Ragon Institute of MGH, MIT and Harvard, Cambridge, Massachusetts, USA
[4]Department of Medicine, Massachusetts General Hospital, Harvard Medical School, Boston, Massachusetts, USA
[5]University of Pittsburgh Medical Center, Pittsburgh, Pennsylvania, USA
[6]Africa Health Research Institute, KwaZulu-Natal, South Africa
[7]Broad Institute, Cambridge, Massachusetts, USA
[8]Santa Fe Institute, Santa Fe, New Mexico, USA

AUTHOR ORCIDs

Tin Phan http://orcid.org/0000-0001-9998-8263
Ruy M. Ribeiro http://orcid.org/0000-0002-3988-8241
Jatin M. Vyas http://orcid.org/0000-0002-9985-9565
Amy K. Barczak http://orcid.org/0000-0003-3806-2381
Alan S. Perelson http://orcid.org/0000-0002-2455-0002

FUNDING

Funder	Grant(s)	Author(s)
HHS | National Institutes of Health (NIH)	U54-HL143541-04	Ruy M. Ribeiro
DOE | NNSA | Los Alamos National Laboratory (LANL)	20200743ER, 20210730ER	Ruy M. Ribeiro
DOE | NNSA | Los Alamos National Laboratory (LANL)	20200695ER	Alan S. Perelson
DOE | NNSA | Los Alamos National Laboratory (LANL)	20220791PRD2	Tin Phan
Massachusetts Consortium on Pathogen Readiness (MCPR)		Jonathan Z. Li Mark J. Siedner Amy K. Barczak

Funder	Grant(s)	Author(s)
Massachusetts General Hospital Department of Medicine		Jatin M. Vyas Mark J. Siedner Amy K. Barczak
HHS | National Institutes of Health (NIH)	U19-AI110818	Jonathan Z. Li Mark J. Siedner Amy K. Barczak Jacob E. Lemieux
HHS | National Institutes of Health (NIH)	R01 AI176287	Jonathan Z. Li Mark J. Siedner Amy K. Barczak Jacob E. Lemieux

AUTHOR CONTRIBUTIONS

Tin Phan, Conceptualization, Formal analysis, Investigation, Methodology, Resources, Software, Validation, Visualization, Writing – original draft, Writing – review and editing | Ruy M. Ribeiro, Conceptualization, Formal analysis, Funding acquisition, Investigation, Methodology, Project administration, Resources, Software, Supervision, Validation, Writing – review and editing | Gregory E. Edelstein, Data curation, Resources, Validation, Writing – review and editing | Julie Boucau, Data curation, Resources, Validation, Writing – review and editing | Rockib Uddin, Data curation, Resources, Writing – review and editing | Caitlin Marino, Data curation, Resources, Writing – review and editing | May Y. Liew, Data curation, Resources, Writing – review and editing | Mamadou Barry, Data curation, Resources, Writing – review and editing | Manish C. Choudhary, Data curation, Resources, Validation, Writing – review and editing | Dessie Tien, Data curation, Resources, Writing – review and editing | Karry Su, Data curation, Resources, Writing – review and editing | Zahra Reynolds, Data curation, Resources, Writing – review and editing | Yijia Li, Data curation, Resources, Writing – review and editing | Shruti Sagar, Data curation, Resources, Writing – review and editing | Tammy D. Vyas, Data curation, Resources, Writing – review and editing | Yumeko Kawano, Data curation, Resources, Writing – review and editing | Jeffrey A. Sparks, Data curation, Resources, Validation, Writing – review and editing | Sarah P. Hammond, Data curation, Resources, Writing – review and editing | Zachary Wallace, Data curation, Resources, Writing – review and editing | Jatin M. Vyas, Data curation, Resources, Writing – review and editing | Jonathan Z. Li, Data curation, Funding acquisition, Resources, Supervision, Validation, Writing – review and editing | Mark J. Siedner, Data curation, Funding acquisition, Project administration, Resources, Supervision, Validation, Writing – review and editing | Amy K. Barczak, Data curation, Funding acquisition, Project administration, Resources, Supervision, Validation, Writing – review and editing | Jacob E. Lemieux, Data curation, Funding acquisition, Project administration, Supervision, Validation, Writing – review and editing | Alan S. Perelson, Conceptualization, Formal analysis, Funding acquisition, Investigation, Methodology, Project administration, Resources, Supervision, Validation, Writing – review and editing

DATA AVAILABILITY

The de-identified viral load data are provided in the supplemental material (SM Data). Codes for fitting, plotting, and *in silico* analyses are available at https://github.com/tinphan-LANL/A-general-code-for-analyzing-viral-load-in-acute-respiratory-infection.

ETHICS APPROVAL

This study was approved by the Massachusetts General Brigham Institutional Review Board, protocol # 2021P000812, and all participants provided informed consent.

REFERENCES

1. 2024. Fact Sheet for Healthcare Providers: Emergency Use Authorization for Paxlovid 2024. Available from: https://www.fda.gov/media/155050/download
2. Hammond J, Leister-Tebbe H, Gardner A, Abreu P, Bao W, Wisemandle W, Baniecki M, Hendrick VM, Damle B, Simón-Campos A, Pypstra R, Rusnak JM, EPIC-HR Investigators. 2022. Oral nirmatrelvir for high-risk, nonhospitalized adults with Covid-19. N Engl J Med 386:1397–1408. https://doi.org/10.1056/NEJMoa2118542
3. Arbel R, Wolff Sagy Y, Hoshen M, Battat E, Lavie G, Sergienko R, Friger M, Waxman JG, Dagan N, Balicer R, Ben-Shlomo Y, Peretz A, Yaron S, Serby D, Hammerman A, Netzer D. 2022. Nirmatrelvir use and severe Covid-19 outcomes during the omicron surge. N Engl J Med 387:790–798. https://doi.org/10.1056/NEJMoa2204919
4. Wong CKH, Au ICH, Lau KTK, Lau EHY, Cowling BJ, Leung GM. 2022. Real-world effectiveness of molnupiravir and nirmatrelvir plus ritonavir against mortality, hospitalisation, and in-hospital outcomes among community-dwelling, ambulatory patients with confirmed SARS-CoV-2 infection during the omicron wave in Hong Kong: an observational study. Lancet 400:1213–1222. https://doi.org/10.1016/S0140-6736(22)01586-0
5. Charness ME, Gupta K, Stack G, Strymish J, Adams E, Lindy DC, Mohri H, Ho DD. 2022. Rebound of SARS-CoV-2 infection after nirmatrelvir-ritonavir treatment. N Engl J Med 387:1045–1047. https://doi.org/10.1056/NEJMc2206449
6. Edelstein GE, Boucau J, Uddin R, Marino C, Liew MY, Barry M, Choudhary MC, Gilbert RF, Reynolds Z, Li Y, Tien D, Sagar S, Vyas TD, Kawano Y, Sparks JA, Hammond SP, Wallace Z, Vyas JM, Barczak AK, Lemieux JE, Li JZ, Siedner MJ. 2023. SARS-CoV-2 virologic rebound with nirmatrelvir–ritonavir therapy: an observational study. Ann Intern Med 176:1577–1585. https://doi.org/10.7326/M23-1756
7. Boucau J, Uddin R, Marino C, Regan J, Flynn JP, Choudhary MC, Chen G, Stuckwisch AM, Mathews J, Liew MY, Singh A, Reynolds Z, Iyer SL, Chamberlin GC, Vyas TD, Vyas JM, Turbett SE, Li JZ, Lemieux JE, Barczak AK, Siedner MJ. 2023. Characterization of virologic rebound following nirmatrelvir-ritonavir treatment for coronavirus disease 2019 (COVID-19). Clin Infect Dis 76:e526–e529. https://doi.org/10.1093/cid/ciac512
8. Duan Y, Zhou H, Liu X, Iketani S, Lin M, Zhang X, Bian Q, Wang H, Sun H, Hong SJ, Culbertson B, Mohri H, Luck MI, Zhu Y, Liu X, Lu Y, Yang X, Yang K, Sabo Y, Chavez A, Goff SP, Rao Z, Ho DD, Yang H. 2023. Molecular mechanisms of SARS-CoV-2 resistance to nirmatrelvir. Nature 622:376–382. https://doi.org/10.1038/s41586-023-06609-0
9. Iketani S, Mohri H, Culbertson B, Hong SJ, Duan Y, Luck MI, Annavajhala MK, Guo Y, Sheng Z, Uhlemann A-C, Goff SP, Sabo Y, Yang H, Chavez A, Ho DD. 2023. Multiple pathways for SARS-CoV-2 resistance to nirmatrelvir. Nature 613:558–564. https://doi.org/10.1038/s41586-022-05514-2
10. Tamura TJ, Choudhary MC, Deo R, Yousuf F, Gomez AN, Edelstein GE, Boucau J, Glover OT, Barry M, Gilbert RF, et al. 2024. Emerging SARS-CoV-2 Resistance After Antiviral Treatment. JAMA Network Open 7:e2435431. https://doi.org/10.1001/jamanetworkopen.2024.35431
11. Soares H, Baniecki ML, Cardin R, Leister-Tebbe H, Zhu Y, Guan S, Hyde C, He W, Wang Z, Hao L, Perrin BS, Bao W, Chan P, Damle B, Menon S, Hammond J, Anderson A. 2022. Viral load rebound in placebo and nirmatrelvir-ritonavir treated COVID-19 patients is not associated with recurrence of severe disease or mutations. In Review. https://doi.org/10.21203/rs.3.rs-1720472/v2
12. Carlin AF, Clark AE, Chaillon A, Garretson AF, Bray W, Porrachia M, Santos AT, Rana TM, Smith DM. 2023. Virologic and immunologic characterization of coronavirus disease 2019 recrudescence after nirmatrelvir/ritonavir treatment. Clin Infect Dis 76:e530–e532. https://doi.org/10.1093/cid/ciac496
13. Epling BP, Rocco JM, Boswell KL, Laidlaw E, Galindo F, Kellogg A, Das S, Roder A, Ghedin E, Kreitman A, Dewar RL, Kelly SEM, Kalish H, Rehman T, Highbarger J, Rupert A, Kocher G, Holbrook MR, Lisco A, Manion M, Koup RA, Sereti I. 2023. Clinical, virologic, and immunologic evaluation of symptomatic coronavirus disease 2019 rebound following nirmatrelvir/ritonavir treatment. Clin Infect Dis 76:573–581. https://doi.org/10.1093/cid/ciac663
14. Tamura TJ. 2024. Analysis of emergent SARS-CoV-2 antiviral resistance and its association with virological rebound. Abstract 135,. Conference on Retroviruses and Opportunistic Infections; Denver, CO. https://www.croiwebcasts.org/p/2024croi/croi/135.
15. Zuckerman NS, Bucris E, Keidar-Friedman D, Amsalem M, Brosh-Nissimov T. 2024. Nirmatrelvir resistance-*de novo* E166V/L50V mutations in an immunocompromised patient treated with prolonged nirmatrelvir/ritonavir monotherapy leading to clinical and virological treatment failure-a case report. Clin Infect Dis 78:352–355. https://doi.org/10.1093/cid/ciad494
16. Hirotsu Y, Kobayashi H, Kakizaki Y, Saito A, Tsutsui T, Kawaguchi M, Shimamura S, Hata K, Hanawa S, Toyama J, Miyashita Y, Omata M. 2023. Multidrug-resistant mutations to antiviral and antibody therapy in an immunocompromised patient infected with SARS-CoV-2. Med 4:813–824. https://doi.org/10.1016/j.medj.2023.08.001
17. Anderson AS, Caubel P, Rusnak JM, EPIC-HR Trial Investigators. 2022. Nirmatrelvir-ritonavir and viral load rebound in Covid-19. N Engl J Med 387:1047–1049. https://doi.org/10.1056/NEJMc2205944
18. Ranganath N, O'Horo JC, Challener DW, Tulledge-Scheitel SM, Pike ML, O'Brien M, Razonable RR, Shah A. 2023. Rebound phenomenon after nirmatrelvir/ritonavir treatment of coronavirus disease 2019 (COVID-19) in high-risk persons. Clin Infect Dis 76:e537–e539. https://doi.org/10.1093/cid/ciac481
19. Dai EY, Lee KA, Nathanson AB, Leonelli AT, Petros BA, Brock-Fisher T, Dobbins ST, MacInnis BL, Capone A, Littlehale N, Boucau J, Marino C, Barczak AK, Sabeti PC, Springer M, Stephenson KE. 2022. Viral kinetics of severe acute respiratory syndrome coronavirus 2 (SARS-CoV-2) omicron infection in mRNA-vaccinated individuals treated and not treated with nirmatrelvir-ritonavir. medRxiv:2022.08.04.22278378. https://doi.org/10.1101/2022.08.04.22278378
20. Wong CKH, Lau KTK, Au ICH, Lau EHY, Poon LLM, Hung IFN, Cowling BJ, Leung GM. 2023. Viral burden rebound in hospitalised patients with COVID-19 receiving oral antivirals in Hong Kong: a population-wide retrospective cohort study. Lancet Infect Dis 23:683–695. https://doi.org/10.1016/S1473-3099(22)00873-8
21. Wang L, Berger NA, Davis PB, Kaelber DC, Volkow ND, Xu R. 2022. COVID-19 rebound after Paxlovid and Molnupiravir during January-June 2022. medRxiv:2022.06.21.22276724. https://doi.org/10.1101/2022.06.21.22276724
22. Smith-Jeffcoat SE, Biddle JE, Talbot HK, Morrissey KG, Stockwell MS, Maldonado Y, McLean HQ, Ellingson KD, Bowman NM, Asturias E, et al. 2024. Symptoms, viral loads, and rebound among COVID-19 outpatients treated with nirmatrelvir/ritonavir compared with propensity score-matched untreated individuals. Clin Infect Dis 78:1175–1184. https://doi.org/10.1093/cid/ciad696
23. Kueper J, Kottilil K, Quer G, Chiang D, Spencer E, Purushotham J, Ramos E, Roumani L, Andersen K, Topol E, Pandit J, Mina M. 2024 Coronavirus disease 2019 rebound in nirmatrelvir plus ritonavir treatment and control groups: a prospective cohort study. In Review. https://doi.org/10.21203/rs.3.rs-5368863/v1
24. Hay JA, Kissler SM, Fauver JR, Mack C, Tai CG, Samant RM, Connolly S, Anderson DJ, Khullar G, MacKay M, Patel M, Kelly S, Manhertz A, Eiter I, Salgado D, Baker T, Howard B, Dudley JT, Mason CE, Nair M, Huang Y, DiFiori J, Ho DD, Grubaugh ND, Grad YH. 2022. Quantifying the impact of immune history and variant on SARS-CoV-2 viral kinetics and infection rebound: a retrospective cohort study. Elife 11:e81849. https://doi.org/10.7554/eLife.81849
25. Deo R, Choudhary MC, Moser C, Ritz J, Daar ES, Wohl DA, Greninger AL, Eron JJ, Currier JS, Hughes MD, Smith DM, Chew KW, Li JZ, ACTIV-2/A5401 Study Team. 2023. Symptom and viral rebound in untreated SARS-CoV-2 infection. Ann Intern Med 176:348–354. https://doi.org/10.7326/M22-2381
26. Pandit JA, Radin JM, Chiang DC, Spencer EG, Pawelek JB, Diwan M, Roumani L, Mina MJ. 2023. The coronavirus disease 2019 rebound study: a prospective cohort study to evaluate viral and symptom rebound differences in participants treated with nirmatrelvir plus ritonavir versus untreated controls. Clin Infect Dis 77:25–31. https://doi.org/10.1093/cid/ciad102
27. Wong G-H, Yip T-F, Lai M-M, Wong V-S, Hui D-C, Lui G-Y. 2022. Incidence of viral rebound after treatment with nirmatrelvir-ritonavir and molnupiravir. JAMA Network Open 5:e2245086. https://doi.org/10.1001/jamanetworkopen.2022.45086
28. Ke R, Martinez PP, Smith RL, Gibson LL, Mirza A, Conte M, Gallagher N, Luo CH, Jarrett J, Zhou R, et al. 2022. Daily longitudinal sampling of

SARS-CoV-2 infection reveals substantial heterogeneity in infectiousness. Nat Microbiol 7:640–652. https://doi.org/10.1038/s41564-022-01105-z
29. Iyaniwura SA, Ribeiro RM, Zitzmann C, Phan T, Ke R, Perelson AS. 2024. The kinetics of SARS-CoV-2 infection based on a human challenge study. Proc Natl Acad Sci U S A 121:e2406303121. https://doi.org/10.1073/pnas.2406303121
30. Kim KS, Ejima K, Iwanami S, Fujita Y, Ohashi H, Koizumi Y, Asai Y, Nakaoka S, Watashi K, Aihara K, Thompson RN, Ke R, Perelson AS, Iwami S. 2021. A quantitative model used to compare within-host SARS-CoV-2, MERS-CoV, and SARS-CoV dynamics provides insights into the pathogenesis and treatment of SARS-CoV-2. PLOS Biol 19:e3001128. https://doi.org/10.1371/journal.pbio.3001128
31. Cao Y, Gao W, Caro L, Stone JA. 2021. Immune-viral dynamics modeling for SARS-CoV-2 drug development. Clin Transl Sci 14:2348–2359. https://doi.org/10.1111/cts.13099
32. Owens K, Esmaeili S, Schiffer JT. 2024. Heterogeneous SARS-CoV-2 kinetics due to variable timing and intensity of immune responses. JCI Insight 9:e176286. https://doi.org/10.1172/jci.insight.176286
33. Goyal A, Cardozo-Ojeda EF, Schiffer JT. 2020. Potency and timing of antiviral therapy as determinants of duration of SARS-CoV-2 shedding and intensity of inflammatory response. Sci Adv 6:eabc7112. https://doi.org/10.1126/sciadv.abc7112
34. Gonçalves A, Bertrand J, Ke R, Comets E, de Lamballerie X, Malvy D, Pizzorno A, Terrier O, Rosa Calatrava M, Mentré F, Smith P, Perelson AS, Guedj J. 2020. Timing of antiviral treatment initiation is critical to reduce SARS-CoV-2 viral load. CPT Pharmacometrics Syst Pharmacol 9:509–514. https://doi.org/10.1002/psp4.12543
35. Czuppon P, Débarre F, Gonçalves A, Tenaillon O, Perelson AS, Guedj J, Blanquart F. 2021. Success of prophylactic antiviral therapy for SARS-CoV-2: predicted critical efficacies and impact of different drug-specific mechanisms of action. PLOS Comput Biol 17:e1008752. https://doi.org/10.1371/journal.pcbi.1008752
36. Hernandez-Vargas EA, Velasco-Hernandez JX. 2020. In-host mathematical modelling of COVID-19 in humans. Annu Rev Control 50:448–456. https://doi.org/10.1016/j.arcontrol.2020.09.006
37. Du Z, Wang L, Bai Y, Liu Y, Lau EHY, Galvani AP, Krug RM, Cowling BJ, Meyers LA. 2024. A retrospective cohort study of Paxlovid efficacy depending on treatment time in hospitalized COVID-19 patients. Elife 13:e89801. https://doi.org/10.7554/eLife.89801
38. Goyal A, Reeves DB, Cardozo-Ojeda EF, Schiffer JT, Mayer BT. 2021. Viral load and contact heterogeneity predict SARS-CoV-2 transmission and super-spreading events. Elife 10:e63537. https://doi.org/10.7554/eLife.63537
39. Korosec CS, Wahl LM, Heffernan JM. 2024. Within-host evolution of SARS-CoV-2: how often are *de novo* mutations transmitted from symptomatic infections? Virus Evol 10:veae006. https://doi.org/10.1093/ve/veae006
40. Esmaeili S, Owens K, Wagoner J, Polyak SJ, White JM, Schiffer JT. 2024. A unifying model to explain frequent SARS-CoV-2 rebound after nirmatrelvir treatment and limited prophylactic efficacy. Nat Commun 15:5478. https://doi.org/10.1038/s41467-024-49458-9
41. Phan T, Zitzmann C, Chew KW, Smith DM, Daar ES, Wohl DA, Eron JJ, Currier JS, Hughes MD, Choudhary MC, Deo R, Li JZ, Ribeiro RM, Ke R, Perelson AS, for the ACTIV-2/A5401 Study Team. 2024. Modeling the emergence of viral resistance for SARS-CoV-2 during treatment with an anti-spike monoclonal antibody. PLOS Pathog 20:e1011680. https://doi.org/10.1371/journal.ppat.1011680
42. Chiarelli A, Dobrovolny H. 2024. Viral rebound after antiviral treatment: a mathematical modeling study of the role of antiviral mechanism of action. Interdiscip Sci Comput Life Sci 16:844–853. https://doi.org/10.1007/s12539-024-00643-w
43. Perelson AS, Ribeiro RM, Phan T. 2023. An explanation for SARS-CoV-2 rebound after Paxlovid treatment. medRxiv:2023.05.30.23290747. https://doi.org/10.1101/2023.05.30.23290747
44. Cao B, Wang Y, Lu H, Huang C, Yang Y, Shang L, Chen Z, Jiang R, Liu Y, Lin L, et al. 2024. Oral simnotrelvir for adult patients with mild-to-moderate Covid-19. N Engl J Med 390:230–241. https://doi.org/10.1056/NEJMoa2301425
45. Yang X-M, Yang Y, Yao B-F, Ye P-P, Xu Y, Peng S-P, Yang Y-M, Shu P, Li P-J, Li S, et al. 2023. A first-in-human phase 1 study of simnotrelvir, A 3CL-like protease inhibitor for treatment of COVID-19, in healthy adult subjects. Eur J Pharm Sci 191:106598. https://doi.org/10.1016/j.ejps.2023.106598
46. Yang Z, Xu Y, Zheng R, Ye L, Lv G, Cao Z, Han R, Li M, Zhu Y, Cao Q, et al. 2024. COVID-19 rebound after VV116 vs nirmatrelvir-ritonavir treatment: a randomized clinical trial. JAMA Network Open 7:e241765. https://doi.org/10.1001/jamanetworkopen.2024.1765
47. Cao Z, Gao W, Bao H, Feng H, Mei S, Chen P, Gao Y, Cui Z, Zhang Q, Meng X, Gui H, Wang W, Jiang Y, Song Z, Shi Y, Sun J, Zhang Y, Xie Q, Xu Y, Ning G, Gao Y, Zhao R. 2023. VV116 versus nirmatrelvir-ritonavir for oral treatment of Covid-19. N Engl J Med 388:406–417. https://doi.org/10.1056/NEJMoa2208822
48. Ke R, Zitzmann C, Ho DD, Ribeiro RM, Perelson AS. 2021. *In vivo* kinetics of SARS-CoV-2 infection and its relationship with a person's infectiousness. Proc Natl Acad Sci U S A 118:e2111477118. https://doi.org/10.1073/pnas.2111477118
49. Wagstaffe HR, Thwaites RS, Reynaldi A, Sidhu JK, McKendry R, Ascough S, Papargyris L, Collins AM, Xu J, Lemm N-M, Siggins MK, Chain BM, Killingley B, Kalinova M, Mann A, Catchpole A, Davenport MP, Openshaw PJM, Chiu C. 2024. Mucosal and systemic immune correlates of viral control after SARS-CoV-2 infection challenge in seronegative adults. Sci Immunol 9:eadj9285. https://doi.org/10.1126/sciimmunol.adj9285
50. Malireddi RKS, Sharma BR, Kanneganti T-D. 2024. Innate immunity in protection and pathogenesis during coronavirus infections and COVID-19. Annu Rev Immunol 42:615–645. https://doi.org/10.1146/annurev-immunol-083122-043545
51. Sette A, Sidney J, Crotty S. 2023. T cell responses to SARS-CoV-2. Annu Rev Immunol 41:343–373. https://doi.org/10.1146/annurev-immunol-101721-061120
52. Savan R, Gale M. 2023. Innate immunity and interferon in SARS-CoV-2 infection outcome. Immunity 56:1443–1450. https://doi.org/10.1016/j.immuni.2023.06.018
53. Schuh L, Markov PV, Veliov VM, Stilianakis NI. 2024. A mathematical model for the within-host (re)infection dynamics of SARS-CoV-2. Math Biosci 371:109178. https://doi.org/10.1016/j.mbs.2024.109178
54. Chatterjee B, Singh Sandhu H, Dixit NM. 2022. Modeling recapitulates the heterogeneous outcomes of SARS-CoV-2 infection and quantifies the differences in the innate immune and CD8 T-cell responses between patients experiencing mild and severe symptoms. PLOS Pathog 18:e1010630. https://doi.org/10.1371/journal.ppat.1010630
55. Samuel CE. 2001. Antiviral actions of interferons. Clin Microbiol Rev 14:778–809, https://doi.org/10.1128/CMR.14.4.778-809.2001
56. Talemi SR, Höfer T. 2018. Antiviral interferon response at single - cell resolution. Immunol Rev 285:72–80. https://doi.org/10.1111/imr.12699
57. Voigt EA, Swick A, Yin J. 2016. Rapid induction and persistence of paracrine-induced cellular antiviral states arrest viral infection spread in A549 cells. Virology (Auckl) 496:59–66. https://doi.org/10.1016/j.virol.2016.05.019
58. García-Sastre A, Biron CA. 2006. Type 1 interferons and the virus-host relationship: a lesson in détente. Science 312:879–882. https://doi.org/10.1126/science.1125676
59. Samuel CE, Knutson GS. 1982. Mechanism of interferon action. Kinetics of decay of the antiviral state and protein phosphorylation in mouse fibroblasts treated with natural and cloned interferons. J Biol Chem 257:11796–11801. https://doi.org/10.1016/S0021-9258(18)33834-1
60. Pawelek KA, Huynh GT, Quinlivan M, Cullinane A, Rong L, Perelson AS. 2012. Modeling within-host dynamics of influenza virus infection including immune responses. PLOS Comput Biol 8:e1002588. https://doi.org/10.1371/journal.pcbi.1002588
61. De Boer RJ, Oprea M, Antia R, Murali-Krishna K, Ahmed R, Perelson AS. 2001. Recruitment times, proliferation, and apoptosis rates during the CD8$^+$ T-cell response to lymphocytic choriomeningitis virus. J Virol 75:10663–10669. https://doi.org/10.1128/JVI.75.22.10663-10669.2001
62. Burnham KP, Anderson DR. 1998. Practical use of the information-theoretic approach, p 75–117. In Model selection and inference. Springer New York, New York, NY.
63. Wong CKH, Lau JJ, Au ICH, Lau KTK, Hung IFN, Peiris M, Leung GM, Wu JT. 2023. Optimal timing of nirmatrelvir/ritonavir treatment after COVID-19 symptom onset or diagnosis: target trial emulation. Nat Commun 14:8377. https://doi.org/10.1038/s41467-023-43706-0
64. Cohen MS, Brown ER. 2023. Rebound of COVID-19 with nirmatrelvir-ritonavir antiviral therapy. Ann Intern Med 176:1672–1673. https://doi.org/10.7326/M23-2887
65. Frediani JK, Parsons R, McLendon KB, Westbrook AL, Lam W, Martin G, Pollock NR. 2024. The new normal: delayed peak SARS-CoV-2 viral loads relative to symptom onset and implications for COVID-19 testing

programs. Clin Infect Dis 78:301–307. https://doi.org/10.1093/cid/ciad582
66. Yang Y, Guo L, Yuan J, Xu Z, Gu Y, Zhang J, Guan Y, Liang J, Lu H, Liu Y. 2023. Viral and antibody dynamics of acute infection with SARS-CoV-2 Omicron variant (B.1.1.529): a prospective cohort study from Shenzhen, China. Lancet Microbe 4:e632–e641. https://doi.org/10.1016/S2666-5247(23)00139-8
67. Zhou K, Hu B, Zhao X, Chi H, Pan J, Zheng Y, Bi X, Chen M, Xie J, Xu J, Tung T-H, Shen B, Zhu H. 2022. Longitudinal observation of viral load in patients infected with Omicron variant and its relationship with clinical symptoms. Front Microbiol 13:1037733. https://doi.org/10.3389/fmicb.2022.1037733
68. Wang Y, Chen X, Xiao W, Zhao D, Feng L. 2022. Rapid COVID-19 rebound in a severe COVID-19 patient during 20-day course of Paxlovid. J Infect 85:e134–e136. https://doi.org/10.1016/j.jinf.2022.08.012
69. Centers for Disease Control and Prevention (U.S.). 2022. COVID-19 rebound after paxlovid treatment 2022. Available from: https://stacks.cdc.gov/view/cdc/117609
70. Fumagalli V, Di Lucia P, Ravà M, Marotta D, Bono E, Grassi S, Donnici L, Cannalire R, Stefanelli I, Ferraro A, Esposito F, Pariani E, Inverso D, Montesano C, Delbue S, Perlman S, Tramontano E, De Francesco R, Summa V, Guidotti LG, Iannacone M. 2023. Nirmatrelvir treatment of SARS-CoV-2-infected mice blunts antiviral adaptive immune responses. EMBO Mol Med 15:e17580. https://doi.org/10.15252/emmm.202317580
71. Carlin AF, Clark AE, Garretson AF, Bray W, Porrachia M, Santos AT, Rana TM, Chaillon A, Smith DM. 2023. Neutralizing antibody responses after severe acute respiratory syndrome coronavirus 2 BA.2 and BA.2.12.1 infection do not neutralize BA.4 and BA.5 and can be blunted by nirmatrelvir/ritonavir treatment. Open Forum Infect Dis 10:ofad154. https://doi.org/10.1093/ofid/ofad154
72. Weinstein E. 2024. Extended nirmatrelvir/ritonavir treatment durations for immunocompromised patients with COVID-19. Poster 00658. Conference on Retroviruses and Opportunistic Infections, Denver, CO
73. Nair MS, Luck MI, Huang Y, Sabo Y, Ho DD. 2024. Persistence of an infectious form of SARS-CoV-2 after protease inhibitor treatment of permissive cells *in vitro*. J Infect Dis:jiae385. https://doi.org/10.1093/infdis/jiae385
74. Yotsuyanagi H, Ohmagari N, Doi Y, Yamato M, Bac NH, Cha BK, Imamura T, Sonoyama T, Ichihashi G, Sanaki T, Tsuge Y, Uehara T, Mukae H. 2024. Efficacy and safety of 5-day oral ensitrelvir for patients with mild to moderate COVID-19: the SCORPIO-SR randomized clinical trial. JAMA Network Open 7:e2354991. https://doi.org/10.1001/jamanetworkopen.2023.54991
75. Shimizu R, Sonoyama T, Fukuhara T, Kuwata A, Matsuo Y, Kubota R. 2022. Safety, tolerability, and pharmacokinetics of the novel antiviral agent ensitrelvir fumaric acid, a SARS-CoV-2 3CL protease inhibitor, in healthy adults. Antimicrob Agents Chemother 66:e0063222. https://doi.org/10.1128/aac.00632-22
76. Vellas C, Kamar N, Izopet J. 2022. Resistance mutations in SARS-CoV-2 omicron variant after tixagevimab-cilgavimab treatment. J Infect 85:e162–e163. https://doi.org/10.1016/j.jinf.2022.07.014
77. Vellas C, Trémeaux P, Del Bello A, Latour J, Jeanne N, Ranger N, Danet C, Martin-Blondel G, Delobel P, Kamar N, Izopet J. 2022. Resistance mutations in SARS-CoV-2 omicron variant in patients treated with sotrovimab. Clin Microbiol Infect 28:1297–1299. https://doi.org/10.1016/j.cmi.2022.05.002
78. Jensen B, Luebke N, Feldt T, Keitel V, Brandenburger T, Kindgen-Milles D, Lutterbeck M, Freise NF, Schoeler D, Haas R, Dilthey A, Adams O, Walker A, Timm J, Luedde T. 2021. Emergence of the E484K mutation in SARS-COV-2-infected immunocompromised patients treated with bamlanivimab in Germany. Lancet Reg Health Eur 8:100164. https://doi.org/10.1016/j.lanepe.2021.100164
79. Choudhary MC, Chew KW, Deo R, Flynn JP, Regan J, Crain CR, Moser C, Hughes MD, Ritz J, Ribeiro RM, et al. 2022. Emergence of SARS-CoV-2 escape mutations during Bamlanivimab therapy in a phase II randomized clinical trial. Nat Microbiol 7:1906–1917. https://doi.org/10.1038/s41564-022-01254-1
80. Peiffer-Smadja N, Bridier-Nahmias A, Ferré VM, Charpentier C, Garé M, Rioux C, Allemand A, Lavallée P, Ghosn J, Kramer L, Descamps D, Yazdanpanah Y, Visseaux B. 2021. Emergence of E484K mutation following bamlanivimab monotherapy among high-risk patients infected with the alpha variant of SARS-CoV-2. Viruses 13:1642. https://doi.org/10.3390/v13081642
81. Liberti DC, Kremp MM, Liberti WA 3rd, Penkala IJ, Li S, Zhou S, Morrisey EE. 2021. Alveolar epithelial cell fate is maintained in a spatially restricted manner to promote lung regeneration after acute injury. Cell Rep 35:109092. https://doi.org/10.1016/j.celrep.2021.109092
82. Bridges JP, Vladar EK, Huang H, Mason RJ. 2022. Respiratory epithelial cell responses to SARS-CoV-2 in COVID-19. Thorax 77:203–209. https://doi.org/10.1136/thoraxjnl-2021-217561
83. Fang Y, Liu H, Huang H, Li H, Saqi A, Qiang L, Que J. 2020. Distinct stem/progenitor cells proliferate to regenerate the trachea, intrapulmonary airways and alveoli in COVID-19 patients. Cell Res 30:705–707. https://doi.org/10.1038/s41422-020-0367-9
84. Killingley B, Mann AJ, Kalinova M, Boyers A, Goonawardane N, Zhou J, Lindsell K, Hare SS, Brown J, Frise R, et al. 2022. Safety, tolerability and viral kinetics during SARS-CoV-2 human challenge in young adults. Nat Med 28:1031–1041. https://doi.org/10.1038/s41591-022-01780-9
85. Gunawardana M, Webster S, Rivera S, Cortez JM, Breslin J, Pinales C, Buser C, Ibarrondo FJ, Yang OO, Bobardt M, Gallay PA, Adler AP, Ramirez CM, Anton PA, Baum MM. 2022. Early SARS-CoV-2 dynamics and immune responses in unvaccinated participants of an intensely sampled longitudinal surveillance study. Commun Med 2:129. https://doi.org/10.1038/s43856-022-00195-4
86. Zitzmann C, Ke R, Ribeiro RM, Perelson AS. 2024. How robust are estimates of key parameters in standard viral dynamic models? PLOS Comput Biol 20:e1011437. https://doi.org/10.1371/journal.pcbi.1011437
87. Ciupe SM, Tuncer N. 2022. Identifiability of parameters in mathematical models of SARS-CoV-2 infections in humans. Sci Rep 12:14637. https://doi.org/10.1038/s41598-022-18683-x
88. Kissler SM, Fauver JR, Mack C, Tai CG, Breban MI, Watkins AE, Samant RM, Anderson DJ, Metti J, Khullar G, Baits R, MacKay M, Salgado D, Baker T, Dudley JT, Mason CE, Ho DD, Grubaugh ND, Grad YH. 2021. Viral dynamics of SARS-CoV-2 variants in vaccinated and unvaccinated persons. N Engl J Med 385:2489–2491. https://doi.org/10.1056/NEJMc2102507
89. Puhach O, Meyer B, Eckerle I. 2023. SARS-CoV-2 viral load and shedding kinetics. Nat Rev Microbiol 21:147–161. https://doi.org/10.1038/s41579-022-00822-w
90. Boucau J, Marino C, Regan J, Uddin R, Choudhary MC, Flynn JP, Chen G, Stuckwisch AM, Mathews J, Liew MY, et al. 2022. Duration of shedding of culturable virus in SARS-CoV-2 omicron (BA.1) infection. N Engl J Med 387:275–277. https://doi.org/10.1056/NEJMc2202092
91. Baccam P, Beauchemin C, Macken CA, Hayden FG, Perelson AS. 2006. Kinetics of influenza A virus infection in humans. J Virol 80:7590–7599. https://doi.org/10.1128/JVI.01623-05
92. Saenz RA, Quinlivan M, Elton D, Macrae S, Blunden AS, Mumford JA, Daly JM, Digard P, Cullinane A, Grenfell BT, McCauley JW, Wood JLN, Gog JR. 2010. Dynamics of influenza virus infection and pathology. J Virol 84:3974–3983. https://doi.org/10.1128/JVI.02078-09
93. Diamond MS, Lambris JD, Ting JP, Tsang JS. 2022. Considering innate immune responses in SARS-CoV-2 infection and COVID-19. Nat Rev Immunol 22:465–470. https://doi.org/10.1038/s41577-022-00744-x
94. Dixit NM, Perelson AS. 2004. Complex patterns of viral load decay under antiretroviral therapy: influence of pharmacokinetics and intracellular delay. J Theor Biol 226:95–109. https://doi.org/10.1016/j.jtbi.2003.09.002
95. Smith AP, Moquin DJ, Bernhauerova V, Smith AM. 2018. Influenza virus infection model with density dependence supports biphasic viral decay. Front Microbiol 9:1554. https://doi.org/10.3389/fmicb.2018.01554
96. PubChem. Nirmatrelvir. Available from: https://pubchem.ncbi.nlm.nih.gov/compound/155903259. Retrieved 07 Mar 2024.